

Lawrence Berkeley National Laboratory

LBL Publications

Title

Generation of high-quality electron beams from a laser-based advanced accelerator**Supported by 973 National Basic Research Program of China (2013CBA01504) and Natural Science Foundation of China NSFC (11121504, 11334013, 11175119, 11374209)

Permalink

<https://escholarship.org/uc/item/0947k7gj>

Journal

Chinese Physics C, 39(6)

ISSN

1674-1137

Authors

Elsied, Ahmed MM
Hafz, Nasr AM
Li, Song
et al.

Publication Date

2015-06-01

DOI

10.1088/1674-1137/39/6/067003

Peer reviewed

PAPER

Generation of high-quality electron beams from a laser-based advanced accelerator

To cite this article: Ahmed M. M. Elsied *et al* 2015 *Chinese Phys. C* **39** 067003

View the [article online](#) for updates and enhancements.

Related content

- [Counter-crossing injection for stable high-quality electron beam generation via laser-plasma interaction](#)
H Kotaki, I Daito, Y Hayashi et al.
- [Lasers target the nucleus](#)
Peter Rodgers
- [0.56 GeV Laser Electron Acceleration in Ablative-Capillary-Discharge Plasma Channel](#)
Takashi Kameshima, Wei Hong, Kiyohiro Sugiyama et al.

Generation of high-quality electron beams from a laser-based advanced accelerator^{*}

Ahmed M. M. Elsied Nasr A. M. Hafz¹⁾ LI Song(李松) Mohammad Mirzaie
Thomas Sokollik ZHANG Jie(张杰)²⁾

Key Laboratory for Laser Plasmas (MOE) and Department of Physics & Astronomy,
Shanghai Jiao Tong University, Shanghai 200240, China

Abstract: At Shanghai Jiao Tong University (SJTU) we have established a research laboratory for advanced acceleration research based on high-power lasers and plasma technologies. In a primary experiment based on the laser wakefield acceleration (LWFA) scheme, multi-hundred MeV electron beams of reasonable quality are generated using 20–40 TW, 30 femtosecond laser pulses interacting independently with helium, neon, nitrogen and argon gas jet targets. The laser-plasma interaction conditions are optimized for stabilizing the electron beam generation from each type of gas. The electron beam pointing angle stability and divergence angle as well as the energy spectra from each gas jet are measured and compared.

Key words: laser wakefield acceleration, electron beam, gas jet, terawatt laser

PACS: 52.38.Kd, 41.75.Jv, 52.35.Mw **DOI:** 10.1088/1674-1137/39/6/067003

1 Introduction

The field of laser-plasma electron acceleration has attracted a great deal of attention since the first quasi-monoenergetic electron beam was observed in 2004 [1–3]. In 2013 the generation of multiple GeV electron beams from two experiments was reported [4, 5]. This acceleration scheme was proposed by Tajima and Dawson in 1979 [6] and is called “laser wakefield acceleration” (LWFA). The scheme works as follows: when an ultra-intense ultrashort laser pulse is focused in under-dense gaseous plasma, its ponderomotive force repels the electrons sideward. However, the ions are practically immobile in this interaction due to the ultra-short nature of the laser pulse. As the electrons are attracted back by the ions’ electrostatic field, they overshoot their initial positions, which sets up a large amplitude electrostatic plasma wave in the wake of the ultra-intense laser pulse [7, 8]. The phase velocity of the plasma wave is equal to the group velocity of the laser pulse in the under-dense plasma, which is almost the speed of light c . If the laser intensity is of the order of 10^{18} W/cm² or higher, and the plasma density is of the order of 10^{18} cm⁻³, the wake’s electrostatic field is of the order of 100 GV/m [9]. Therefore, the LWFA scheme has the potential to be the basis for a new technology which could lead to

downsizing future particle accelerators. In order to reach the high intensity required to form the plasma wave, the laser pulse must be tightly focused. This in turn will shorten the interaction length, limited by diffraction to the Rayleigh length ($Z_R = \pi r_o^2/\lambda$) [10], where r_o is the laser spot size and λ is the laser wavelength. Numerous methods had been examined experimentally and by simulation to extend the propagation distance beyond the diffraction limit, most notably preformed channels [11, 12] and relativistically self-guided channels [13, 14].

The propagation of the laser through plasma causes a change in the index of refraction with the radius at high laser power. This can be explained as follows: since the laser intensity changes with radius and the plasma frequency changes with the relativistic mass factor, the index of refraction, which is given by $n = (1 - \omega_p^2/\omega_0^2)^{1/2}$, will also vary with radius [15], where ω_p is the plasma frequency and ω_0 is the laser frequency. Under these conditions, the plasma acts like a positive lens and focuses the beam. This effect has been found to have a power threshold given by $P_c[\text{GW}] = 16.5 n_c/n_e$, where n_e and n_c are the plasma and critical plasma densities, respectively [16]. At laser power of the order of $3P_c$ the beam extends and forms a second focus. With further increase in laser power, multiple foci should occur, and finally merge into a single channel [15].

Received 16 September 2014

^{*} Supported by 973 National Basic Research Program of China (2013CBA01504) and Natural Science Foundation of China NSFC (11121504, 11334013, 11175119, 11374209)

1) E-mail: nasr@sjtu.edu.cn (corresponding author)

2) E-mail: jzhang1@sjtu.edu.cn

©2015 Chinese Physical Society and the Institute of High Energy Physics of the Chinese Academy of Sciences and the Institute of Modern Physics of the Chinese Academy of Sciences and IOP Publishing Ltd

In this paper we report on the generation of electron beams from the LWFA scheme in various gases, namely He, Ne, N, and Ar individually. We optimized the laser-plasma interaction conditions for the generation of electron beams of reasonable quality. We investigate Ne gas as a target for the first time. He gas has been used in numerous previous experiments [17–19], while N gas has been less tried [20] and Ar is the least common gas [21] target in LWFA experiments. The aim is the generation of electron beams with low divergence and high pointing stability. The current work could be useful to the ionization injection LWFA scheme [22–25] where a mixture of low- Z gas (e.g. He or H) and high- Z gas (e.g. N or Ar) are commonly used. Therefore, the generation of electron beams and the study of their parameters with each gas individually are meaningful.

2 Experimental setup

A schematic diagram of the experimental setup is shown in Fig. 1. The research was carried out using a newly-installed Ti: Sapphire laser system at the Key Laboratory for Laser Plasmas (LLP) at Shanghai Jiao Tong University in China. The laser system, which is based on the CPA (chirped-pulse amplification) technique, operates at 10 Hz, generating pulses with duration of 30 fs at a wavelength of 800 nm. Though the laser operates at 10 Hz, we performed the experiment at a lower repetition rate, which is necessary for parameter optimization at the current stage of such laser-based accelerators. The maximum peak power of the laser pulses is 200 TW. However, this experiment was the first to use the facility and to avoid unexpected damage to the system, we used only 20–40 TW laser power. The laser pulses were focused onto the gas jet using $f/20$ off-axis parabola (OAP). The focal spot size in vacuum was $30\ \mu\text{m}$ (FWHM), and is shown in Fig. 2. The Rayleigh length based on $(1/e^2)$ radius of the maximum intensity was 2.5 mm. Thus, the peak focused laser intensity and the corresponding normalized vector potential, a_0 , were approximately $(0.7\text{--}2.0)\times 10^{18}\ \text{W}/\text{cm}^2$ and 0.6–1.0, respectively. The shot-to-shot laser energy was measured based on a calibration of the leaked laser en-

ergy measured by an energy meter, as shown in Fig. 1. The electron beam spatial profile on a phosphor screen called DRZ-Mitsubishi Chemical ($\text{Gd}_2\text{O}_2\text{S:Tb}$) was imaged onto a 14-bit charge-coupled device (CCD). The electron beam energy spectrum was measured by moving a dipole magnet into the beam path after the gas jet. The maximum magnetic field intensity was 0.94 T and the 2D-field intensity was mapped using a gauss meter. The magnetic field data points were then used in a relativistic particle trajectory code (written using

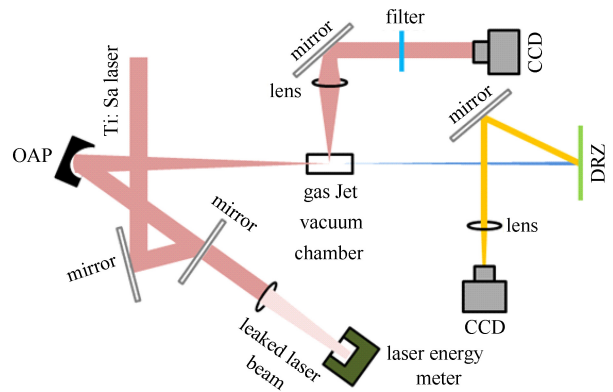


Fig. 1. A schematic diagram of the experimental setup.

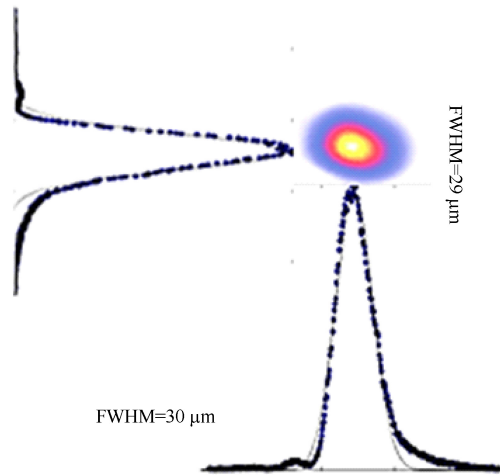


Fig. 2. The focused laser spot.

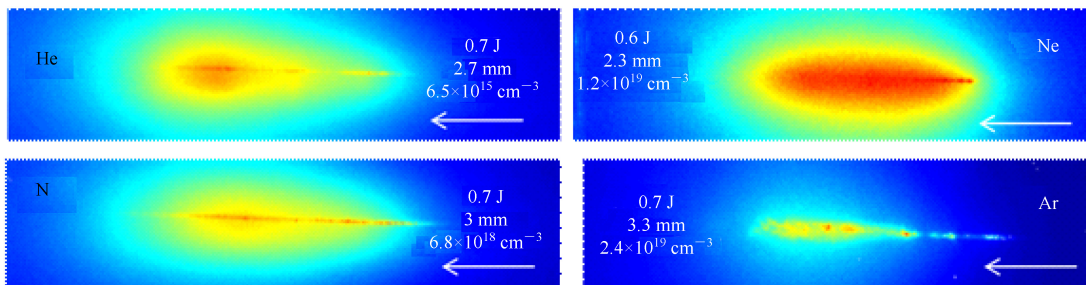


Fig. 3. Images of the laser-plasma channels observed in different gas jets. The laser energy, the length of each channel, the plasma density and the laser direction propagation are shown on each panel.

MATLAB) to calculate the electron beam energy. In the calculation, the beam's pointing angle (based on the data shown in Fig. 4, below) to the magnet entrance plane was taken into account. The laser-plasma interaction volume was imaged from the top by a 14-bit CCD. A narrow band-pass filter with transmission wavelength at ~ 500 nm was used in front of the CCD for collecting only the scattered laser light near the second harmonic wavelength.

3 Experimental results and discussions

A first step toward the observation of an electron beam from a laser-plasma accelerator is to make sure that the laser pulse has been guided during its propagation in the plasma, which means that one has to observe laser-plasma channels. Typical laser-plasma channels captured by the top-view CCD are shown in Fig. 3, where 2.3–3.3 mm long laser-plasma channels were observed. The laser-plasma channels are narrow over the full length, except for the Ar gas jet where the channel starts narrow then expands later on. We believe that such channel behavior in Ar might be a result of cluster formation, which is common in Ar gas jet expansion at atmospheric pressures [26]. In order for laser-plasma accelerators to be used for applications, the electron beam pointing stability has to be dramatically enhanced [27]. Fig. 4 shows the pointing angles of electron beams generated by laser-driven He, Ne, N and Ar gas jets, respectively. The results are shown for different plasma

densities and laser energies. For the case of a helium gas jet, Fig. 4 (a), the electron beam showed quite stable pointing over the plasma density range 6.7×10^{18} – 1.0×10^{19} cm^{-3} , in which the beam pointing deviation from zero pointing was less than 10 mrad in 58% of the laser shots. However, outside the above density range, the beams had larger pointing angles. For the neon gas jet case and in 60% of the laser shots the electron beam had a deviation of 12 mrad over a wide plasma density range of 2×10^{18} – 3.6×10^{19} cm^{-3} , as shown in Fig. 4(b). For the nitrogen gas jet case, the highest (in this experiment) electron beam pointing stability was observed; in 47% of the shots the electron beam had a deviation of only 5 mrad at a plasma density of $\sim 1 \times 10^{18}$ cm^{-3} . Moreover, in 73% of the laser shots the electron beam had deviations less than 10 mrad in the plasma density range of 9.5×10^{17} – 1.5×10^{18} cm^{-3} , Fig. 4(c). Finally, the argon gas jet case showed the lowest reproducibility and electron beam quality (as presented below) over the scanned range of plasma densities, 4.0 – 6.0×10^{18} cm^{-3} . The beam deviation from zero pointing over this plasma density range was less than 15 mrad. A quick conclusion on beam pointing from the above-mentioned gas jets is the following: there is a clear trend for more stable electron beam pointing with small pointing angle fluctuations at low plasma densities. As the density increases the electron beam pointing angles increase. Thus for real applications of LWFA beams we suggest the use of gas jets at as low densities as possible.

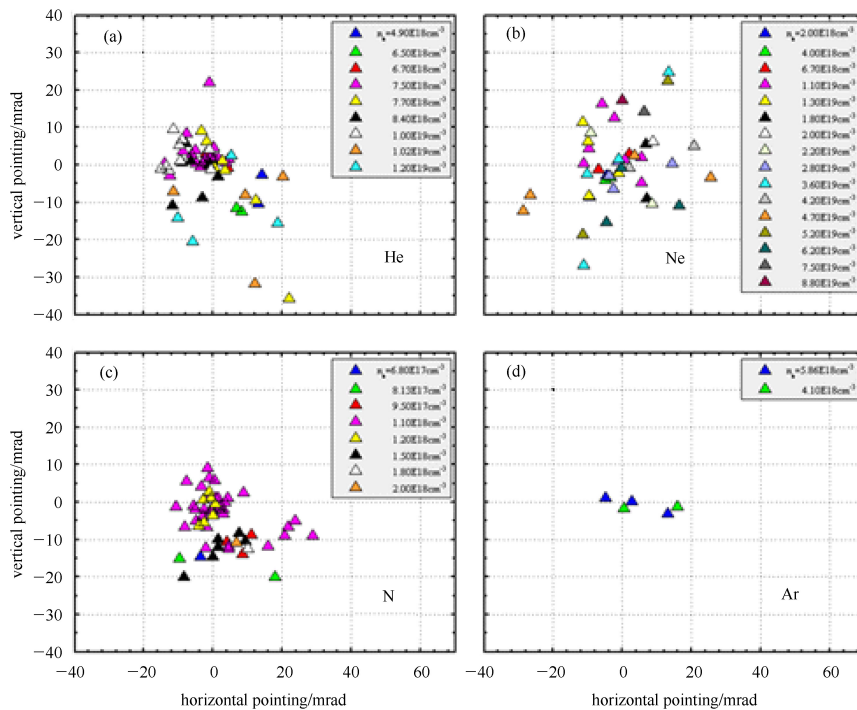


Fig. 4. Electron beam pointing angle in the laser-driven He, Ne, N and Ar gas jet targets at different densities.

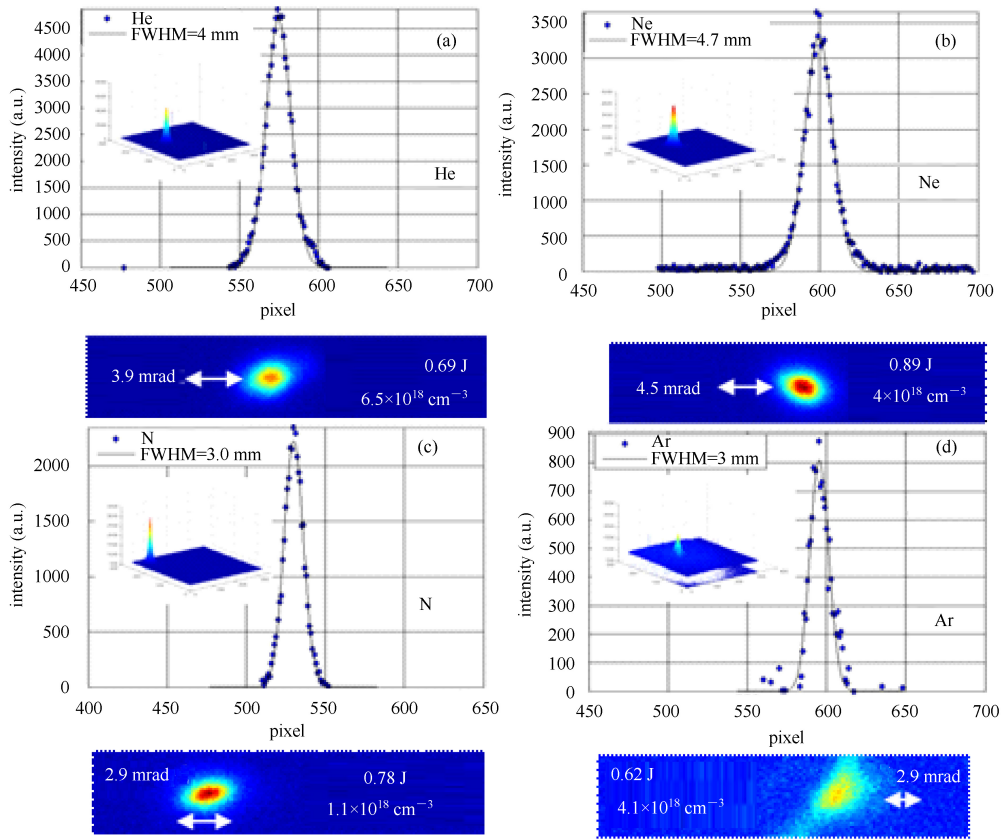


Fig. 5. 2D and 3D spatial profiles of electron beams from laser-driven He, Ne, N, and Ar gas jet targets.

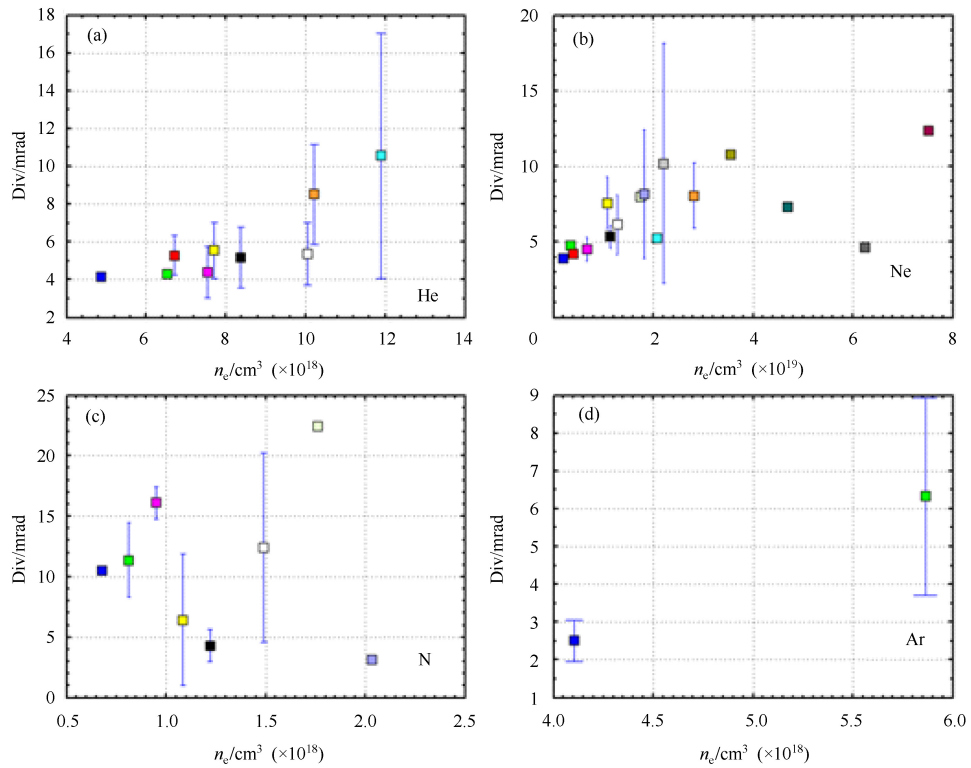


Fig. 6. Electron beam divergence angle (FWHM) dependence on the plasma density for He, Ne, N, and Ar gas jets.

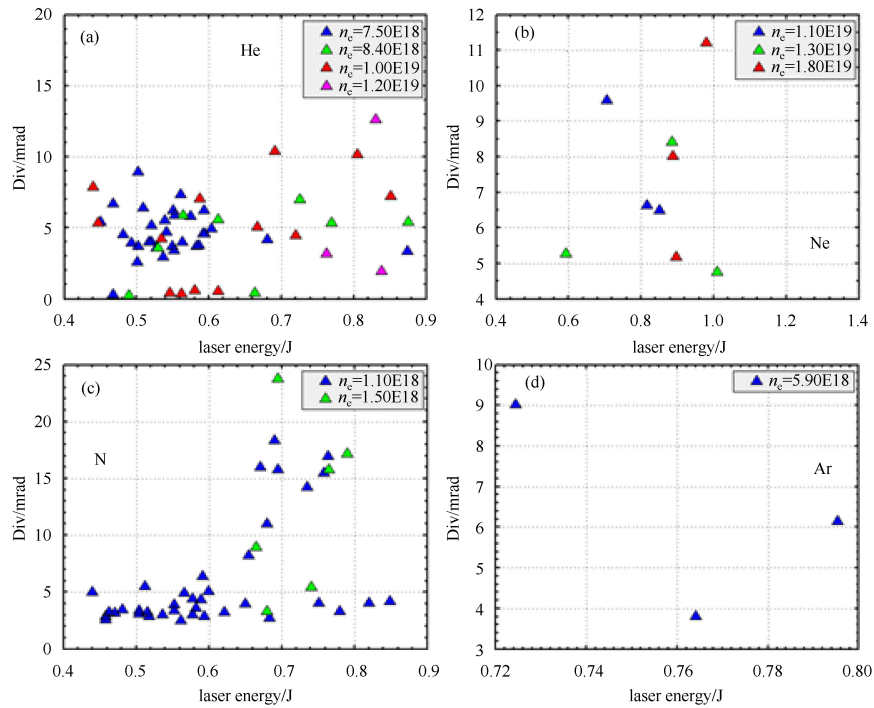


Fig. 7. Electron beam divergence angle (FWHM) dependence on the laser energy for He, Ne, N, and Ar gas jets.

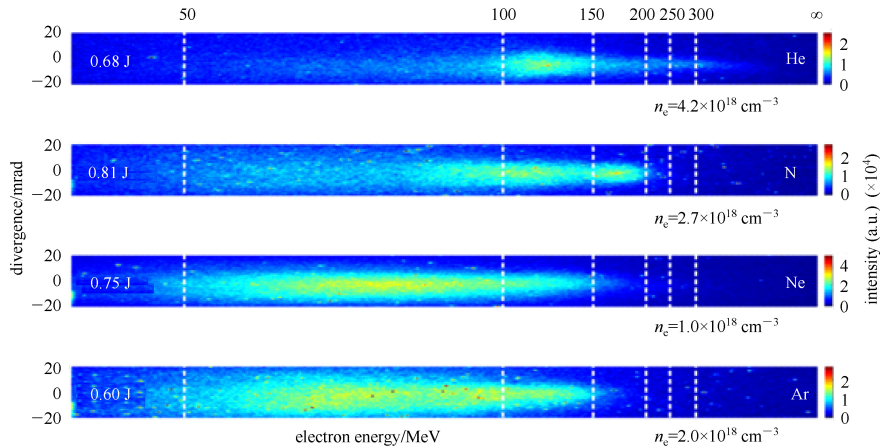


Fig. 8. Electron beam energy spectra from laser-driven He, N, Ne, and Ar gas jets. The plasma density and laser energy are shown for each case.

Figure 5 shows electron beam spatial profiles from the 4 different gas jet targets upon interaction with the laser. Generally, the electron beam brightness was several thousand counts using the 14-bit CCD for all gas jets, except the electron beams from the Ar gas jet, which were relatively weak. Typically, the electron beam divergence (FWHM) was <5 mrad, which is well-collimated high-quality. In Fig. 5 we show the laser energy and the plasma density for each beam profile. We noticed that the beam divergence is sensitive to the plasma density in each gas jet target, as shown in Fig. 6. In the He gas jet case (Fig. 6(a)), the beam divergence shows a clear trend of increasing from 4 mrad at low density to > 10

mrad at the density of $1.2 \times 10^{19} \text{ cm}^{-3}$. A similar trend has been observed for the beams from the laser-driven Ar gas jet (Fig. 6(d)). However, the beam divergence trend of the beams from Ne and H gas jets is an initial increase with density followed by a decrease at high densities (Fig. 6(a)–(c)). Finally, we have observed the electron beam divergence angle versus the laser intensity, Fig. 7. Fig. 7(a), (c) showing clearly that well-collimated beams were generated from the He and N gas jets at a moderate laser energy around 0.5–0.7 J (corresponding to 16–24 TW). In this case, there is a clear trend for a larger beam divergence at higher laser intensities. The trend was unclear for electron beams from the Ne and Ar gas jet cases; we

believe that we need more data in future research to get a clearer conclusion on this issue.

Finally, we recorded the electron beam energy spectra from the 4 different laser-driven gas jets, with the results shown in Fig. 8. Obtained using 23 TW (laser energy of 0.68 J) at a plasma density of $4.2 \times 10^{18} \text{ cm}^{-3}$, the electron beam energy spectrum (top-panel) from the He gas jet shows a quasi-monoenergetic peak at ~ 120 MeV, while the maximum energy extends up to $\gtrsim 300$ MeV. The electron beam from the 27 TW laser-driven N gas jet shows a wider energy spectrum (Fig. 8 2nd panel) with quasi-monoenergetic peaks at ~ 110 MeV and 170 MeV. Electron beam energy spectra from the Ne and Ar gas jets are even wider, with maximum energies around 150 MeV. However, as shown on the CCD counts (which are proportional to the beam yield), the He electron beam yield is lower than all beams generated from the other gas jets at roughly the same laser power. The highest yield was obtained from the Ne and Ar gas jets (3rd and 4th panels of Fig. 8). The obtained energies and energy spectra of Fig. 8 are generally expected; it is known that the electron self-injection mechanism in

laser-driven pure He gas jet generally generates a quasi-monoenergetic spectrum, especially at low plasma density. However, for high- Z gas jets the injection into the wakewave is controlled by the ionization process which generally generates large energy spread (continuous spectrum) beams.

4 Conclusions

We have experimentally generated electron beams from He, Ne, N, and Ar gas jet targets. The properties of the electron beams from each gas jet have been studied and compared. Electron beams from the N gas jet had the lowest divergence (2.9 mrad) and pointing angle (< 5 mrad). However, some electrons from the He gas jet reached 300 MeV of energy. Higher yields are observed in Ne and Ar gas jets.

We appreciate Feng Liu and X. L. Ge for their help on the laser, and the useful discussions with Prof. K. Nakajima.

References

- 1 Faure J, Glinec Y, Pukhov A, Kiselev S, Gordienko S, Lefebvre E, Rousseau J P, Burgy F, Malka V. *Nature*, 2004, **431**: 541
- 2 Geddes C G R, Toth Cs, van Tilborg J, Esarey E, Schroeder C B, Bruhwiler D, Nieter C, Cary J, Leemans W P. *Nature*, 2004, **431**: 538
- 3 Mangles S P D, Murphy C D, Najmudin Z, Thomas A G R, Collier J L, Dangor A E, Divall E J, Foster P S, Gallacher J G, Hooker C J, Jaroszynski D A, Langley A J, Mori W B, Norreys P A, Tsung F S, Viskup R, Walton B R, Krushelnick K. *Nature*, 2004, **431**: 535
- 4 WANG X, Zgadzaaj R, Fazel N, LI Z, YI S A, ZHANG X, Henderson W, CHANG Y Y, Korzekwa R, Tsai H E, Pai C H, Quevedo H, Dyer G, Gaul E, Martinez M, Bernstein A C, Borger T, Spinks M, Donovan M, Khudik V, Shvets G, Ditmire T, Downer M C. *Nature Communications*, 2013, **4**: 1988
- 5 Kim H T, Pae K H, CHA H J, Kim I J, YU T J, Sung J H, Lee S K, Jeong T M, Lee J. *Physical Review Letters*, 2013, **111**: 165002
- 6 Tajima T, Dawson J M. *Physical Review Letters*, 1979, **43**: 267
- 7 Le Blanc S P, Downer M C, Wagner R, CHEN S Y, Maksimchuk A, Mourou G, Umstadter D. *Physical Review Letters*, 1996, **77**: 5381
- 8 Nakajima K, Fisher D, Kawakubo T, Nakanishi H, Ogata A, Kato Y, Kitagawa Y, Kodama R, Mima K, Shiraga H, Suzuki K, Yamakawa K, ZHANG T, Sakawa Y, Shoji T, Nishida Y, Yugami N, Downer M, Tajima T. *Physical Review Letters*, 1995, **74**: 4428
- 9 Esarey E, Schroeder C B, Leemans W P. *Review of Modern Physics*, 2009, **81**: 1229
- 10 Chiron A, Bonnaud G, Dulieu A, Miquel J L, Malka G, Louis Jacquet M, Mainfray G. *Physics of Plasmas*, 1996, **3**: 1373
- 11 Sprangle P, Esarey E, Krall J, Joyce G. *Physical Review Letters*, 1992, **69**: 2200
- 12 Durfee III C G, Lynch J, Milchberg H M. *Physical Review E*, 1995, **51**: 2368
- 13 Max C E, Arons J, Langdon A B. *Physical Review Letters*, 1974, **33**: 209
- 14 Esarey E, Krall J, Sprangle P. *Physical Review Letters*, 1994, **72**: 2887
- 15 Wanger R, CHEN S Y, Maksimchuk A, Umstadter D. *Physical Review Letters*, 1997, **78**: 3125
- 16 Krushelnick K, Ting A, Moore C I, Burris H R, Esarey E, Sprangle P, Baine M. *Physical Review Letters*, 1997, **78**: 4047
- 17 Rao B S, Moorti A, Rathore R, Chakera J A, Naik P A, Gupta P D. *Physical Review Special Topics- Accelerators and Beams*, 2014, **17**: 011301
- 18 Thomas A G R, Najmudin Z, Mangles S P D, Murphy C D, Dangor A E, Kamperidis C, Lancaster K L, Mori W B, Norreys P A, Rozmus W, Krushelnick K. *Physical Review Letters*, 2007, **98**: 095004
- 19 Ben-Ismaïl A, Faure J, Malka V. *Nuclear Instruments and Methods in Physics Research A*, 2011, **629**: 82
- 20 MO M Z, Ali A, Fourmaux S, Lassonde P, Kieffer J C, Fedosejevs R. *Applied Physics Letters*, 2012, **100**: 07410
- 21 Mizuta Y, Hosokai T, Masuda S, Zhidkov A, Makito K, Nakanii N, Kajino S, Nishida A, Kando M, Mori M, Kotaki H, Hayashi Y, Bulanov S V, Kodama R. *Physical Review Special Topics - Accelerators And Beams*, 2012, **15**: 121301
- 22 Pak A, Marsh K A, Martins S F, LU W, Mori W B, Joshi C. *Physical Review Letters*, 2010, **104**: 025003
- 23 Pollock B B, Clayton C E, Ralph J E, Albert F, Davidson A, Divol L, Filip C, Glenzer S H, Herpoldt K, LU W, Marsh K A, Meinecke J, Mori W B, Pak A, Rensink T C, Ross J S, Shaw J, Tynan G R, Joshi C, Froula D H. *Physical Review Letters*, 2011, **107**: 045001
- 24 ZENG Ming, Hafz N A M, Nakajima K, CHEN Li-Ming, LU Wei, Mori W B, SHEN Zheng-Ming, ZHANG Jie. *Journal of Plasma Physics*, 2012, **78**: 363
- 25 ZENG Ming, CHEN Min, SHENG Zheng-Ming, Mori W B, ZHANG Jie. *Physics of Plasmas*, 2014, **21**: 030701
- 26 Hagen O F. *Z. Phys. D - Atoms, Molecules and Clusters*, 1990, **17**: 157
- 27 Hafz N A M, YU T J, Lee S K, Jeong T M, Sung J H, Lee J. *Applied Physics Express*, 2010, **3**: 076401